Visual Analysis of TerraSAR-X Backscatter Imagery for Archaeological Prospection

Roland Linck, München, Thomas Busche & Stefan Buckreuss, Wessling

Summary: The use of satellite radar widens the possibilities of archaeological prospection extremely. The resolution of the available sensors however was quite limited until now and only the detection of huge upstanding monuments or cultural landscapes was possible. The launch of TerraSAR-X, a German radar satellite in 2007, however, now offers a resolution of up to 1 m, which is required as a minimum for detecting small archaeological remains. Whereas upstanding monuments are clearly identifiable, it was still uncertain, whether the used high-frequency X-band waves of TerraSAR-X could penetrate the soil and provide information on buried archaeology as well. This paper shows the results of two test sites in Syria and Italy. Both of them have in common that there are extensive surveys by ground-based geophysical surveys with magnetometry and ground-penetrating radar, which provide information on the buried archaeological remains. By a detailed visual comparison of these results with the TerraSAR-X data, we can prove that there is a slight penetration depth of a few decimetres.

Zusammenfassung: *Visuelle Analyse von Terra-SAR-X-Daten für die archäologische Prospektion.* Durch die Verwendung von Satellitenradar erweitern sich die Einsatzmöglichkeiten der archäologischen Prospektion enorm. Die geringe Auflösung der bisher verfügbaren Sensoren ließ jedoch nur eine Prospektion von großen obertägigen Bauwerken und Kulturlandschaften zu. Mit dem Start von TerraSAR-X, einem deutschen Radarfernerkundungssatelliten im Jahr 2007 ist nun eine Auflösung von bis zu 1 m möglich, die mindestens notwendig ist, um auch kleinere archäologische Befunde zu visualisieren. Während sich obertägige Befunde deutlich im Radargramm abzeichnen, war immer noch unklar, ob die hochfrequenten X-Band-Wellen von TerraSAR-X in den Boden eindringen und somit Informationen über die untertägige Archäologie liefern können. Dieser Artikel zeigt die Resultate von zwei Testflächen in Syrien und Italien, die diese Vermutung bestätigen. Von beiden liegen aufgrund großflächiger bodenbasierter Messungen mit Magnetometer und Bodenradar ausführliche Aussagen über die untertägige Archäologie vor. Der detaillierte visuelle Vergleich dieser Ergebnisse mit den TerraSAR-X-Daten zeigt, dass eine gewisse Eindringtiefe von einigen Dezimetern in den Boden zu erwarten ist.

1 Introduction

A new era in remote sensing by synthetic aperture radar (SAR) started by the launch of the German satellite TerraSAR-X in 2007. The first attempts to use SAR as a tool in the field of archaeological prospection were already made in the 1980s, shortly after the first SAR images by the satellite SEASAT were available. These results could only prove the existence of huge ancient remains like paleochannels, drainage systems and former cultural landscapes (Adams 1980, Adams et al. 1981, Adams 1982, McCauley et al. 1982, Walker 1982, Pope & Dahlin 1989, Holcomb 1990, Holcomb 1992a, Holcomb 1992b, Holcomb & Allan 1992, Sever 1998). The reason for this was the limited resolution of the first sensors. Smaller archaeological anomalies could hence not be identified. Therefore, also Blom (1992) could only prove the existence of the lost town of Ubar (Oman) by several converging roads in the desert, but not by distinct remains of buildings. Newer research results on

archaeological prospection with SAR have been conducted in Italy (PIRO et al. 2011), Iraq and Sudan (PATRUNO et al. 2012), and Italy and North Africa (STEWART et al. 2012). The main problem of all these attempts was the limited spatial resolution of several metres, which made it necessary to apply special filter techniques like the H/α-decomposition. In contrast to that, the presented work is done with TerraSAR-X, which allows a spatial resolution of up to 1 m. Hence, the detection of small archaeological remains is possible. In distinction to the published results on SAR studies by other sensors (COMER & BLOM 2007, CHEN et al. 2012, TILTON & COMER 2012), the presented work was done by the visual analysis of identifiable linear archaeological remains in the TerraSAR-X amplitude images. The main effort of the presented study lies on the research on a potential penetration depth of the high-frequency X-band waves of TerraSAR-X into the soil. The detected buried linear archaeological features are afterwards verified by the results of ground-based geophysical surveys.

2   Data and Methods

2.1 *Ground-based Geophysical Methods*

For comparison and to verify the buried archaeological remains at the presented two test sites in Syria and Italy additional ground-based geophysical surveys with magnetometry and ground-penetrating radar (GPR) were carried out. While the measurements in Ostia were executed by HELMUT BECKER of the Bavarian State Department of Monuments and Sites (BLfD) in Munich, the one in Qreiye has been conducted by SIRRI SEREN of the Central Institute for Meteorology and Geodynamics (ZAMG) in Vienna, Austria.

Magnetometer prospecting

Magnetometry is a successful and cost-effective tool for the detailed mapping of large areas in a reasonable time (ENGLISH HERITAGE 2008). For our purpose and in order to reach the highest possible sensitivity combined with a maximum speed of prospection, the so-called "duo-sensor" configuration (FASS-BINDER 2010) was chosen. The probes are here mounted on a wooden frame and carried in a zigzag-mode 30 cm above the ground. The profiles are oriented approximately east-west in order to minimize technical disturbances of the magnetometer probes. The Scintrex Smartmag SM4G Special magnetometer provides a measurement of the geomagnetic field with sensitivity of $\pm$ 10 pT; for comparison: the value of the geomagnetic field, e.g. in Palmyra in March 1997, has been 45,440 $\pm$ 30 nT. For archaeological sites, normally around 90% of the magnetometer data has an anomaly of $\pm$ 10 nT. All measured features with stronger magnetization are due to burnt archaeological remains or pieces of iron (FASSBINDER & GORKA 2009).

Ground-penetrating radar

Ground-penetrating-radar (GPR) is an active geophysical method. It is based on electromagnetic waves propagating in the subsurface dependent on frequency, conductivity and dielectric properties of the material. At discontinuities, where these properties are changing, the radar waves are partially reflected (CONY-ERS 2004). Therefore, GPR is best for locating subsurface stonewalls and burnt brick walls. The soil parameters and the centre frequency of the antenna also determine the maximum penetration depth of the signal. A rule of thumb is that the signal penetrates deeper at a lower frequency, but these antennas have lower resolution. Hence, always a compromise between resolution and penetration depth has to be found. For archaeological purposes, antennas with a centre frequency between 400 and 900 MHz provide the best conditions. By registering the GPR data in three dimensions, it is possible to generate time or depth slices of variable thickness to show the exact depth structure of an archaeological object. This depicts a great advantage compared to magnetometer prospection.

2.2 *Space-borne Radar*

For the presented SAR surveys, the TerraSAR-X satellite (TSX) was used. TSX car-
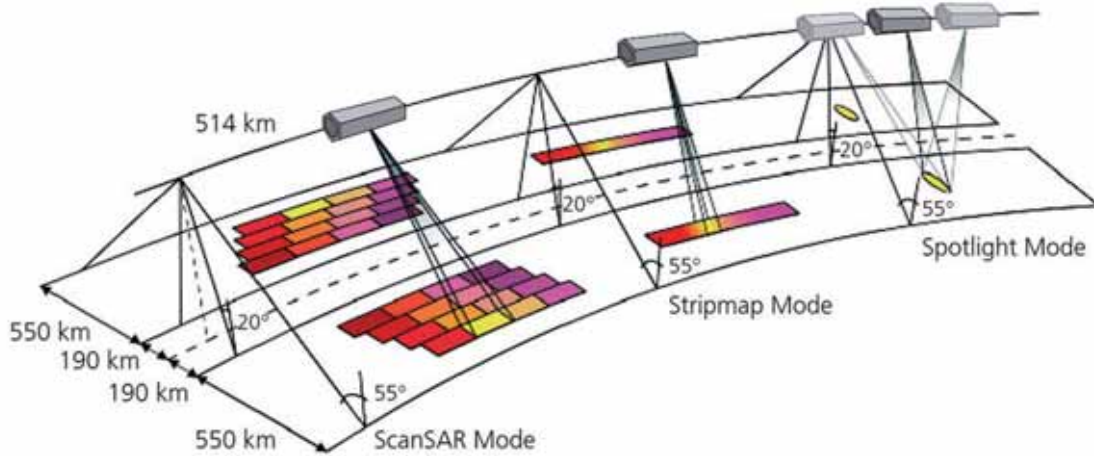
Fig. 1: TerraSAR-X offers three acquisition modes: Stripmap, ScanSAR and Spotlight; all of them are right- and left-looking. The acquisition mode determines the possible resolution and swath width (© DLR).

Tab. 1: Parameters of the TerraSAR-X Strip-map-mode (DLR 2009b).

Swath width	30 km (single polarized) 15 km (dual polarized)
Product length	50 km
Azimuth resolution	3.3 m (single polarized) 6.6 m (dual polarized)
Horizontal resolution	1.7 m – 3.5 m
Polarisation	HH or VV (single polarized) HH/VV, HH/HV, VV/VH (dual polarized)

Tab. 2: Parameters of the TerraSAR-X Scan-SAR-mode (DLR 2009b).

Number of combined strips	4
Swath width	100 km
Product length	150 km
Azimuth resolution	18.5 m
Horizontal resolution	1.7 m – 3.5 m
Polarisation	HH or VV (single polarized)

ries a high frequency X-band SAR sensor that can be operated in three different modes and various polarizations. The Spotlight-, Strip-map- and ScanSAR-modes provide high-resolution images for a detailed analysis as well as wide swath data whenever a larger coverage is required (Fig. 1). The Stripmap-mode is the standard acquisition mode for SAR data and the typical inclination angles are between 20° and 60° (DLR 2009a, b). The parameters of TSX in Stripmap-mode can be seen in Tab. 1. The reduced swath width for dual polarization is caused by the doubling of the impulse frequency. Therefore, the DLR offers two data products: "stripNear" and "stripFar".

The ScanSAR-mode is used to overcome the limitations of swath width in Stripmap-mode. This can be done by alternating between swathes with different inclination angles. Whereas this method enables a larger swath width, the azimuth resolution is lowered by the reduction of the Doppler spectra's bandwidth (DLR 2009a, b) (Tab. 2).

In Spotlight-mode the radar beam is steered in flight direction to map a narrow target area with a high resolution (DLR 2009a, b). TSX uses a so-called "sliding-Spotlight"-mode with the steering point far outside of the target area. The different sliding contribution determines resolution and scene size and hence two Spotlight-modes are available (Tabs. 3 & 4). By using the experimental 300 MHz band-

width in the high-resolution Spotlight mode, it is possible to achieve a spatial resolution of 1 m. As for archaeological prospection only comparable small areas, but a very high resolution are required, this mode in a single polarization offers the best conditions. The DLR does not acquire these high-resolution products by default, so they have to be ordered separately within a scientific proposal.

The presented research was done with a time series of nine consecutive high-resolution Spotlight-TSX data takes between February and May 2012 for Qreiye and a single data take of October 2012 for Ostia (see Tab. 5 for further details on the acquisition parameters). All data has been geocoded and ellipsoid corrected to the UTM WGS84 projection. The data correspond to the level 1b data of the TSX mission. The correction is done by an averaged surface height taken of the digital elevation model (DEM) of the shuttle radar topography mission (SRTM). The geometric precision is, as a result of the used high-quality science orbit, ca. 1 m.

The time series of Qreiye, which was acquired with the same parameters, should have only small deviations in the relative location of the single scenes, even though the absolute precision of the location is restricted by the quality of the DEM. Altogether the relative position of the images to each other should be two pixels with a pixel spacing of 0.5 m. The processing uses the first data take of 06/02/2012 as a reference. All other eight acquisitions are resampled by a cubic resampling method to the image bounds and the pixel spacing of this master image and compiled in a multichannel stack. No fine registration, e.g. using pixel correlation techniques, is performed. From this stack different multi-temporal (3, 6 and all 9 dates) average images are calculated by evaluating the unweighted average of the scenes on the base of the radar brightness β_0 under consideration of inclination angle, calibration constant and intensity. The huge advantage of this approach, in comparison to using only a single data take, is the enormously higher signal/noise-ratio of the resulting radar image. This allows a much better identification of the buried linear archaeological structures.

Tab. 3: Parameters of the TerraSAR-X high-resolution Spotlight-mode (DLR 2009b).

Scene size	5 km (azimuth) × 10 km (horizontal)
Azimuth resolution	1.1 m (single polarized) 2.2 m (dual polarized)
Horizontal resolution	1.5 m – 3.5 m
Polarization	HH or VV (single polarized) HH/VV (dual polarized)

Tab. 4: Parameters of the TerraSAR-X Spotlight-mode (DLR 2009b).

Scene size	10 km (azimuth) × 10 km (horizontal)
Azimuth resolution	1.7 m (single polarized) 3.4 m (dual polarized)
Horizontal resolution	1.5 m – 3.5 m
Polarization	HH or VV (single polarized) HH/VV (dual polarized)

Tab. 5: Parameters of the used data acquisitions of TerraSAR-X (SRA = single-receive antenna).

	Date	Beam	Orbit	Incidence angle	Pass direction	Polarization	Antenna receive configuration	Bandwidth
Qreiye	06/02/2012 – 26/05/2012	spot_039	54	34.9°	asc	HH	SRA	300 MHz
Ostia	19/10/2012	spot_048	93	38.7°	desc	HH	SRA	300 MHz

3 Study Sites

In this paper two test sites in Syria and Italy are presented. The first example shows a Roman fortress in Qreiye at the Euphrates River. It is located ca. 12 km northwest of the Syrian provincial capital Deir ez-Zor (Fig. 2a). The fortress was constructed in the early 3rd century AD and only used for around 50 years. Afterwards, it was abandoned and the area was never reconstructed until today (Gschwind & Hasan 2008). Aerial photos and optical satellite images (Fig. 3) show that only the surrounding wall-ditch-system of the fortress can nowadays be identified at the surface as a slight sandy hill. The internal layout of Qreiye is buried under a small layer of sand and can only be visualized by geophysical methods. Therefore, between 2002 and 2005 the whole fortress of ca. 5 ha size has been surveyed with GPR by Sirri Seren from the ZAMG in Vienna with a Sensors & Software PulseEKKO 1000 and a 900 MHz antenna, a GSSI SIR-3000 and a 400 MHz antenna, with Sensors & Software Noggin and a 500 MHz antenna. The GPR profiles have a crossline spacing of 25 cm or 50 cm and are orientated 45° to the archaeological remains to assure the detection of all buried features (Seren et al. 2009). The corresponding depth slices between 0 and 100 cm depth show a typical structure of such Roman fortresses with orthogonal streets (*via decumana* and *via principalis*), official buildings (*principia*), storage buildings (*horrea*) and soldier barracks (Gschwind & Hasan 2008) (Fig. 4).

Our other test site is the Roman harbour in Ostia Antica (Fig. 2b) which is located ca. 25 km from Rome downstream the river Tiber. Only 50% – 60% of the ancient ruins have already been excavated. These can be mainly dated to the harbour city of ancient Rome in the first centuries AD. Ostia existed between the 4th century BC and the 5th century AD. Its zenith was in the 2nd century AD (DAI 2001). In Ostia a magnetometer survey was carried out by Helmut Becker of the BLfD in 1996/97 (Heinzelmann et al. 1997, Becker 1999). The corresponding magnetogram of this part of the Roman city Ostia Antica is characterized by several roads with a high magnetic anomaly due to the pavement with basaltic rocks (Fig. 5). These roads are flanked with adobe wall buildings. Hence, they have a positive magnetization, too. In the south, the remains of the early Roman city wall with a bypass road towards the sea can be identified. Spectacular is the detection of an Early-Christian basilica overlaying the Roman buildings. Consequent excavations proofed that this has been
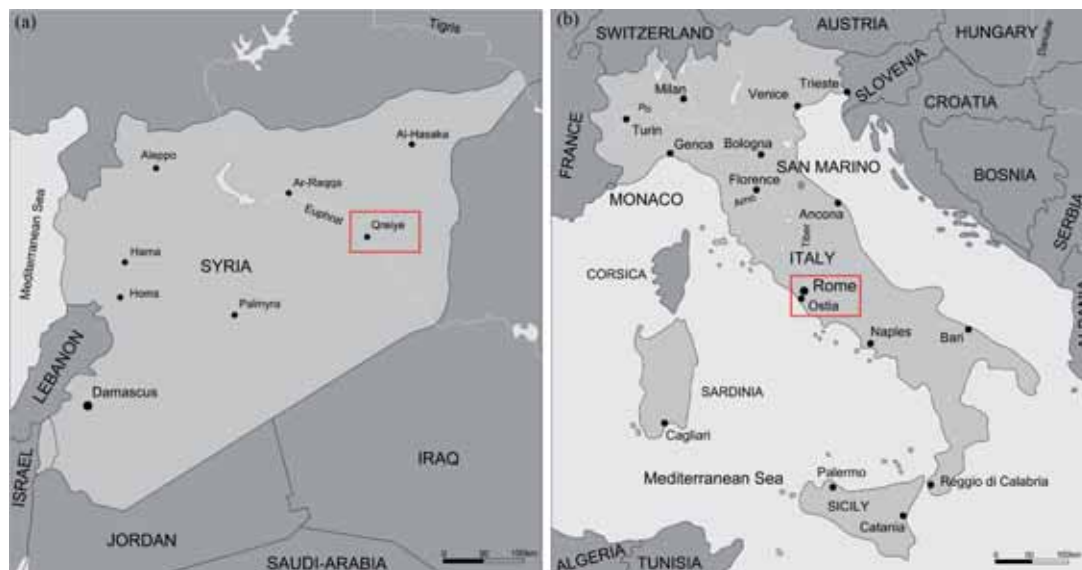
Fig. 2: (a) Topographical map showing the location of the archaeological site Qreiye in Syria; (b) Topographical map of Italy showing Ostia near the capital Rome. The two sites are marked with red rectangles.

the episcopal church founded by the famous emperor Constantine I. Aside of the archaeology, several diffuse, higher magnetic anomalies can be seen. They are caused by the geology; more precisely by the slow sedimentation of shore terraces or fluviatile shore sediments (HEINZELMANN et al. 1997, BECKER 1999).

Fig. 3: Qreiye. Optical satellite image of the fortress by GeoEye's OrbView-3 satellite. Date of data take: 19/03/2005; cloud coverage: 0%; panchromatic image with 1 m spatial resolution (Data available from the U.S. Geological Survey).

Fig. 4: Qreiye. Exemplary depth slice of 20 cm – 30 cm depth. Sensors & Software PulseEK-KO 1000 with 900 MHz antenna, GSSI SIR-3000 with 400 MHz antenna, and Sensors & Software Noggin with 500 MHz antenna; sample interval: 5 cm x 25 cm or 50 cm (after: SEREN et al. 2009).
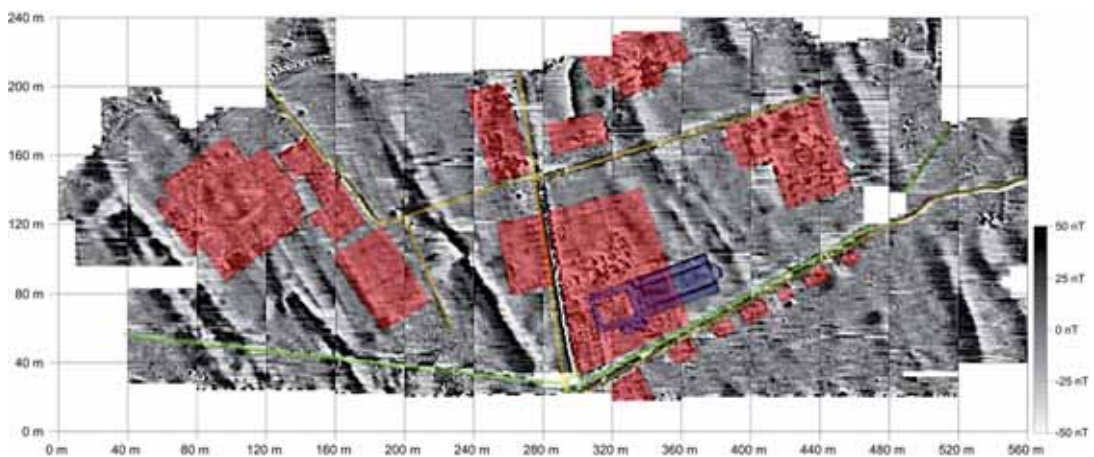
Fig. 5: Ostia. Magnetogram of the survey in the year 1996. Overlay with the high-pass filter to visualize the archaeological remains in more detail and a schematic digital interpretation of the visible features. Colour coding: red = Roman buildings, yellow = Roman roads, green = city wall, blue = Early-Christian basilica. Caesium Smartmag SM4G-Special, Quad-Sensor-configuration, Dynamics: ± 50 nT in 256 greyscales, sensitivity: ±10 pT, point density: 50 cm x 25 cm, interpolated to 25 cm x 25 cm, 40-m-grids (after: BECKER 1999).

4 Results

4.1 *Qreiye*

As, apart from the enclosure wall, no further archaeological remains are visible at the surface, nearly all visible structures in the TerraSAR-X data have to be due to buried archaeology. Of course, also the quite huge remains of the western part of the fortification system can be identified (Fig. 6). The southern and eastern parts have been destroyed by the modern village 'Ayyāš. In the north, no fortification has been erected, as this side has a natural protection by the steep slope towards the Euphrates. Moreover, a huge amount of further linear features can be distinguished in the TerraSAR-X image. The comparison with the GPR depth slices reveals that these structures correspond very well with the enclosure wall and several wall of the internal buildings of the fortress Qreiye (Fig. 6b). The visible walls belong to the central *principia*, several soldier barracks and storage houses. As a result of the still limited resolution of 1 m, not all distinct walls and buildings detected by GPR can be identified. Nevertheless, both methods show a similar layout of the Roman archaeological

remains and the results correspond very well. In addition to the known Roman features, several further structures corresponding to other buildings and the continuation of the fortification wall in the south are visible (LINCK 2013, LINCK et al. 2013). The last one could not be detected by GPR as its grid only covered the interior of the fortress and some small parts of the surrounding areas.

The detailed analysis of the SAR image reveals that the reflections of the basaltic fundaments of the walls cannot be distinguished from the reflections of the mud-bricks like in GPR and both show up mainly as dark anomalies. The reason could be that the reflected signal of both structures cannot reach the sensor anymore. In the case of the stone walls, it could be due to the reflection of the radar waves away from the satellite; the adobe bricks perhaps absorb the signal. In some cases in contrary the signal is backscattered towards the sensor by some parts of the basalt stones (LINCK 2013, LINCK et al. 2013).

The comparison of the TSX radargram with the GPR depth slices reveals that all visible archaeological structures belong to those appearing for the first time in a depth of 20 cm – 30 cm. Every feature lying deeper than
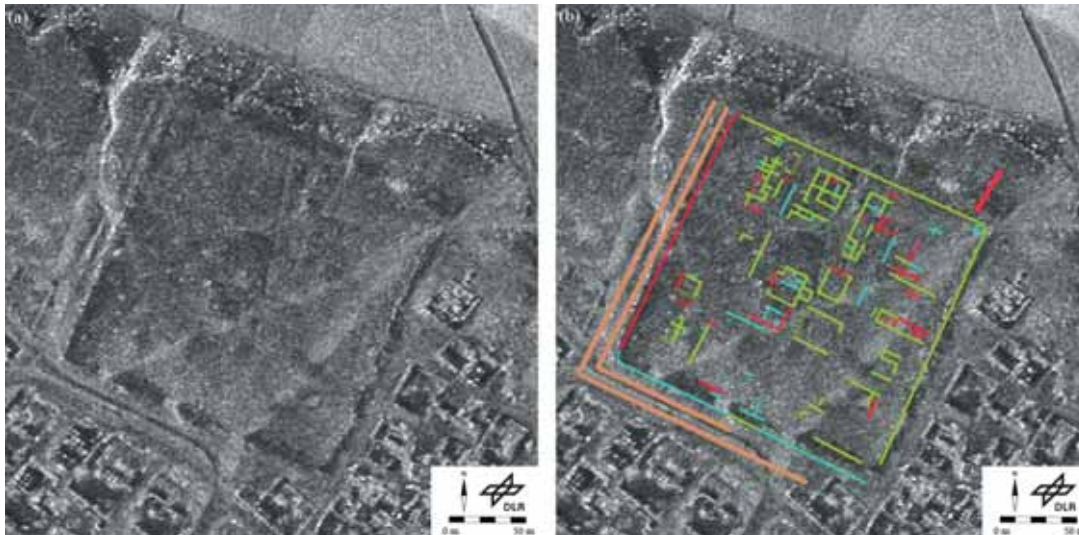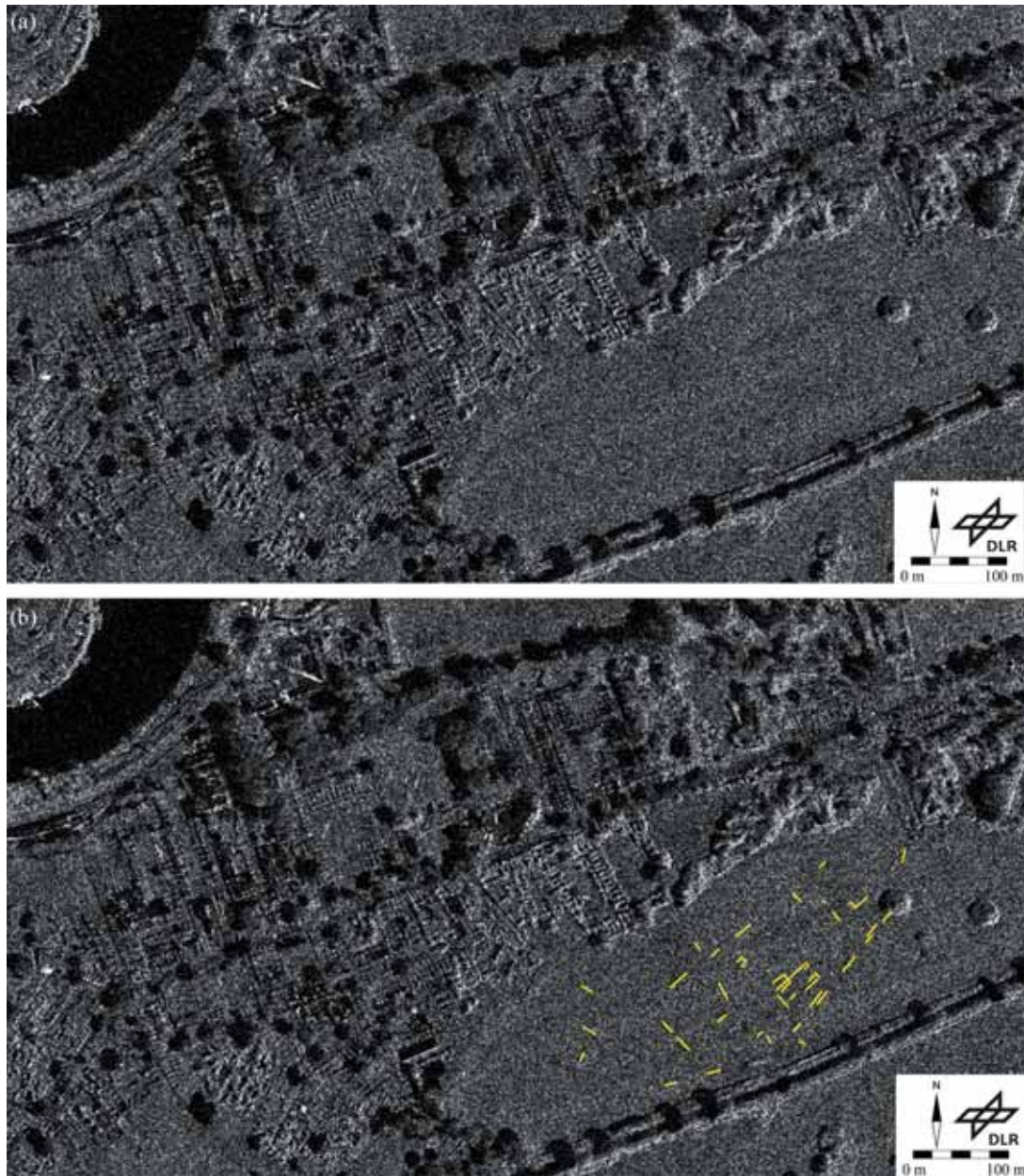

Fig. 6: Qreiye. (a) TerraSAR-X image of the Roman fortress. "High-resolution Spotlight mode" with experimental 300 MHz bandwidth; spatial resolution: 1 m; polarization: horizontal; inclination angle: 34.87°; stacking of all nine data takes; time of data take: February – May 2012 (© DLR 2012). (b) Overlay of the TerraSAR-X image with the digital interpretation of the visible remains. Colour coding: green = GPR result of 10 cm – 20 cm depth; red = GPR result of 20 cm – 30 cm depth; blue = features not mapped with GPR in any depth; brown = superficial remains of the rampart-ditch-system.

30 cm cannot be resolved with TSX. Hence, we can suppose that the X-band waves of the used sensor have a penetration depth of 20 cm – 25 cm in dry desert soil (Linck 2013, Linck et al. 2013). Until now, it was supposed that X-band waves cannot penetrate the soil at all. However, our results in Qreiye indicate that there is a small penetration depth in dry conditions.

4.2 *Ostia*

While the test site in Syria is situated in a dry desert climate and therefore provides very good conditions for the use of SAR to detect buried archaeological remains, the next example is from Italy. As it characterized by a subtropical Mediterranean climate, totally different external conditions can be found.

Fig. 7: Ostia. (a) TerraSAR-X image. "High-resolution Spotlight mode" with experimental 300 MHz bandwidth; spatial resolution: 1 m; polarization: horizontal; inclination angle: 38.7°; data take: 19/10/2012 (© DLR 2012). (b) Overlay of the TerraSAR-X image with the digital interpretation of the visible remains.

At the first glance, in the visually analysed TSX data, the upstanding monuments in the excavated part of Ostia Antica can be detected (Fig. 7). These are mainly the east-west running main road, several residential areas, remains of two huge storage buildings and of some temples and bathes. Because it has been restored in 1940, the theatre of Ostia depicts a very good reflector for the SAR waves, too.

But like in the afore-mentioned two examples, also traces of the buried archaeology can be identified. The following analysis concentrates on the area of the described magnetogram, as a proof of the detected remains can be given there. With TSX, parts of the Roman roads (inside the city, as well as the bypass), parts of the city wall and some walls of the Roman houses can be mapped (Fig. 7b). Whereas the north-south running road in the middle can be seen in the magnetogram very well because of an underlying adobe water pipe (Fig. 5), all roads appear at the same signal strength in the TSX image. The reason is that all road pavements reflect the electromagnetic waves in the same way and the pipeline cannot be visualized by a resolution of 1 m. The best mapped monument in this area is the basilica of Constantine, as it is preserved very well and lays very closes to the surface.

In comparison to the test site in Qreiye, only few buried archaeological features can be identified in Ostia. The reason is the much higher soil moisture in Italy. So the penetration depth of the X-band waves is further reduced and the identification of buried archaeological remains becomes difficult.

5   Conclusion

The results of the two test sites illustrate that even the very high-frequency X-band waves of TerraSAR-X can penetrate the soil and buried features become visible by volume scattering in the ground. A comparison with the GPR depth slices reveals that it is possible to determine a rough estimation on the penetration depth. For dry and sandy desert soils this is approximately 20 cm – 25 cm. For higher soil moisture as well as vegetated ground, the possibility of TSX to resolve buried archaeological features is reduced dramatically. So the method of SAR is best suitable to survey an archaeological site in the desert regions of the world. In these areas often the political situation does not allow ground-based investigations, neither by geophysical methods nor excavations. Hence, remote sensing is the only possibility to collect such data. Because of the short acquisition time, not only the sites themselves, but furthermore even their former cultural landscape can be mapped. So the archaeological remains can be set in a larger context. Due to the still limited resolution of the available SAR sensors of 1 m, afterwards ground-based geophysical measurements with magnetometry or ground-penetrating radar should follow in selected areas to generate an overall image of the site.

The presented results give a first overview on the huge possibilities of satellite radar in the field of archaeological prospection. In the future the gained knowledge will be applied on further test sites with different archaeological and climatic conditions. Another milestone for the use of SAR in archaeological prospection will be the possibility to acquire data in the new Staring-Spotlight-mode of TSX with an enhanced resolution of 25 cm in autumn 2013.

Acknowledgement

References

Adams, R.E.W., 1980: Swamps, Canals, and the Locations of Ancient Maya Cities. – Antiquity **54** (212): 206–214.

ADAMS, R.W.E., BROWN, W.E. & CULBERT, T.P., 1981: Radar Mapping, Archaeology, and Ancient Maya Land Use. – Science **213** (4515): 1457–1463.

ADAMS, R.W.E., 1982: Ancient Maya Canals – Grids and Lattices in the Maya Jungle. – Archaeology **35** (6): 28–35.

BECKER, H., 1999: Prospecting in Ostia Antica (Italy) and the Discovery of the Basilica of Constantinus I. in 1996. – FASSBINDER, J.W.E. & IRLINGER, W.E. (eds.): Archaeological Prospection. – ICOMOS, Hefte des Deutschen Nationalkomitees **33:** 139–143, Karl M. Lipp Verlag, München.

BLOM, R.G., 1992: Space Technology and the Discovery of Ubar, Point of Beginning. – 1992 Data Collector Survey **17** (6): 11.

CHEN, L., COMER, D.C., PRIEBE, C.E., SUSSMAN, D. & TILTON, J.C., 2012: Refinement of a method for identifying probable archaeological sites from remotely sensed data. – COMER, D.C. & HARROWER, M.J. (eds): Mapping Archaeological Landscapes from Space. – Observance of the 40th Anniversary of the World Heritage Convention: 251–258, Springer.

COMER, D.C. & BLOM, R.G., 2007: Detection and identification of archaeological sites and features using synthetic aperture radar (SAR) data collected from airborne platforms. – WISEMAN, J.R. & EL-BAZ, F. (eds.): Remote sensing in archaeology: 103–136, Springer.

CONYERS, L.B., 2004: Ground-Penetrating Radar for Archaeology. – AltaMira Press, Walnut Creek, CA, USA.

DAI, 2001: http://www.ostia-antica.org/ heinzelmann/daiproj.htm (12.3.2013).

DLR, 2009a: TerraSAR-X. Das deutsche Radarauge im All. – Publikationen des Deutschen Zentrums für Luft- und Raumfahrt, Köln.

DLR, 2009b: TerraSAR-X Ground Segment. Basic Product Specification Document, http://www. terrasar-x.dlr.de/ (28.12.2012).

ENGLISH HERITAGE, 2008: Geophysical Survey in Archaeological Field Evaluation. – English Heritage Publications, Swindon, UK.

FASSBINDER, J.W.E., 2010: Geophysikalische Prospektionsmethoden – Chancen für das archäologische Erbe. – EMMERLING, E. (ed.): Toccare – Non Toccare: 10–32, Siegl Verlag, München.

FASSBINDER, J.W.E. & GORKA, T.H., 2009: Beneath the desert soil – archaeological prospecting with a ceasium magnetometer. – REINDEL, M. & WAGNER, G.A. (eds): New technologies for archaeology. Multidisciplinary investigations in Palpa and Nasca, Peru. – First, Natural Science in Archaeology: 49–69, Springer.

GSCHWIND, M. & HASAN, H., 2008: Das römische Kastell Qreiye-'Ayyāš, Provinz Deir ez-Zor, Sy-rien. Ergebnisse des syrisch-deutschen Kooperationsprojektes. – Zeitschrift für Orient-Archäologie **1:** 316–334.

HEINZELMANN, M., BECKER, H., EDER, K. & STEPHANI, M., 1997: Vorbericht zu einer geophysikalischen Prospektionskampagne in Ostia Antica. – Mitteilungen des Deutschen Archäologischen Instituts, Römische Abteilung **104:** 537–548.

HOLCOMB, D.W., 1990: Satellite Imaging to Search for Lost Chinese Cities of the Silk Road. – DAVID, W. (ed.): Spirit of Enterprise: The 1990 Rolex Awards: 260–262, Buri Verlag, Bern, Switzerland.

HOLCOMB, D.W., 1992a: Shuttle Imaging Radar and Archaeological Survey in China's Taklamakan Desert. – Journal of Field Archaeology **19** (1): 129–138.

HOLCOMB, D.W., 1992b: Space Shuttle Eyes Silk Road. – Archaeology **19** (1):129–138.

HOLCOMB, D.W. & ALLAN, J., 1992: Radar Data – An Important Source for the 1990s. – 18th Annual Conference of the Remote Sensing Society: 408–413, Dundee, UK.

LINCK, R., 2013: Methodische Untersuchungen zur Weiterentwicklung der Boden- und Satellitenradarprospektion in der Archäologie. – Shaker Verlag, Aachen.

LINCK, R., BUSCHE, T., BUCKREUSS, S., FASSBINDER, J. & SEREN, S., 2013: Possibilities of archaeological prospection by high-resolution X-band satellite radar – a case study from Syria. – Archaeological Prospection **20** (2): 97–108.

MCCAULEY, J.F., SCHABER, G.G., BREED, C.S., GROLIER, M.J., HAYNES, C.V., ISSAWI, B., ELACHI, C. & BLOM, R., 1982: Subsurface Valleys and Geoarchaeology of the Eastern Sahara Revealed by Shuttle Radar. – Science **218**: 1004–1020.

PATRUNO, J., DORE, N., POTTIER, E. & SARTI, F., 2012: Comparison of polarimetric SAR sensors for archaeological purposes. – 3rd EARSeL Workshop "Advances in Remote Sensing for Archaeology and Cultural Heritage Management" 66, Ghent, Belgium, in press.

PIRO, S., CRESPI, M., DORE, N., PATRUNO, J. & ZAMUNER, D., 2011: Comparison of SAR data, optical satellite images and GPR investigations for archaeological site detection. – 9th International Conference on Archaeological Prospection: 169–171, Izmir, Turkey.

POPE, K.O. & DAHLIN, B.H., 1989: Ancient Maya Wetland Agriculture: New Insights from Ecological and Remote Sensing Research. – Journal of Field Archaeology **16:** 87–106.

SEREN, S., HINTERLEITNER, A., GSCHWIND, M., NEUBAUER, W. & LÖCKER, K., 2009: Combining data of different GPR systems of surveys of the ro-

man fort Qreiye-'Ayyash, Syria. ArcheoScienc-
es **33:** 353–355.

Sever, T.L., 1998: Validating Prehistoric and Cur-
rent Social Phenomena upon the Landscape of
the Peten, Guatemala. – Liverman, D., Moran,
E.F., Rindfuss, R.R. & Stern, P.C. (eds): People
and Pixels: 145–163, National Academy Press,
Washington D.C., USA.

Stewart, C., Lasaponara, R. & Schiavon, G., 2012:
Potential of Quad Pol C-band, Single and Dual
Pol L-band SAR to identify buried archaeology.
– 3rd EARSeL Workshop "Advances in Remote
Sensing for Archaeology and Cultural Heritage
Management" 30, Ghent, Belgium, in press.

Tilton, J.C. & Comer, D.C., 2012: Method for iden-
tifying probable archaeological sites from re-
motely sensed data. – Comer, D.C. & Harrower,
M.J. (eds): Mapping Archaeological Landscapes
from Space. – Observance of the 40th Anniver-
sary of the World Heritage Convention: 241–249,
Springer.

Walker, A.S., 1982: Deserts of China. – American
Scientists **70:** 366–376.

Addresses of the Authors

Dr. Roland Linck, 1.) Bavarian State Department
of Monuments and Sites, Archaeological Prospec-
tion, Hofgraben 4, D-80539 Munich, Germany,
2.) Department. of Earth and Environmental Sci-
ences, Geophysics, Ludwig-Maximilians-Universi-
ty, Theresienstraße 41, D-80333 Munich, Germany,
e-mail: roland.linck@blfd.bayern.de

Thomas Busche, Dr. Stefan Buckreuss, German
Aerospace Centre, Microwaves and Radar Institute,
Münchner Straße 20, D-82234 Wessling, Germany,
e-mail: {thomas.busche}{stefan.buckreuss}@dlr.de